PRELIMINARY ELECTROMAGNETIC SIMULATIONS OF RADAR SCATTERING FROM THE LUNAR SURFACE AS APPLIED TO MINI-RF OBSERVATIONS. M. I. Zimmerman[1], G. W. Patterson[1], D. B. J. Bussey[1], and the Mini-RF Team. [1]Johns Hopkins University Applied Physics Laboratory, Laurel, MD (Michael.Zimmerman@jhuapl.edu)

Introduction: Bistatic radar measurements of the lunar surface are being carried out by the Mini-RF team using Arecibo as a transmitter, cf. Fig. 1. The resulting radar images – the first to be collected at non-zero bistatic phase angle β (between source and receiver) – are being studied extensively to test the hypothesis that water ice resides inside permanently shadowed and perhaps other very cold regions near the lunar poles.

The present work uses electromagnetic simulations to model radar scattering from a Mini-RF lunar "pixel" (on the order of 20 m x 20 m) at wavelength 12.6 cm. We focus on understanding in high detail how properties of the far-field scattered radiation observed by Mini-RF changes with bistatic phase angle, surface roughness, and a plausible variety of inhomogeneous compositions, incl. buried or blocky water ice.

Rationale: Monostatic data (taken at $\beta=0^\circ$) show enhanced circular polarization ratio (CPR, between same- and opposite-polarized components with respect to the source wave) near fresh craters as well as in permanently shadowed "anomalous" craters [1,2,3], which can be interpreted as backscatter from an ice/regolith mix, albeit non-uniquely. Laboratory observations of electromagnetic scattering from lunar regolith samples have also shown elevated backscattered intensity and CPR at $\beta=0^\circ$ [4] but have been limited to only a small handful of available samples.

However, laboratory observations [4,5] and now Mini-RF bistatic data [6] provide access to a wider range of phase angles and suggest that the β-dependence of CPR is sensitive to surface composition. For example, lab observations and theoretical work suggest that CPR drops more precipitously for a water ice target than for mare materials as phase angle β is increased (e.g., Fig. 2).

Electromagnetic finite-difference time-domain (FDTD) simulations have been employed to investigate lunar radar scattering [7], including a variety of polarization effects, but these efforts were limited to incidence angles below about 60° by technical constrants. Mini-RF bistatic data is acquired at incidence angles $> 60^\circ$ for a number of interesting targets (upwards of 85°) and thus FDTD modeling requires a new approach.

Simulation results: We have successfully used a freely-available FDTD package [8] to model the grazing-incidence regime that was inaccessible in previous lunar-relevant efforts. A sample 2D simulation is depicted in Fig. 3, with a plane wave incident from the right upon a featureless 5° dielectric slope ($\varepsilon_r=4+0i$). This models a continuous radar source incident upon a polar area of the Moon. By applying a circularly polarized source wave and varying the slope of the surface we have benchmarked the code against the Fresnel equations (Fig. 4a), providing an important first confirmation of the high physical fidelity of our setup. The grid spacing required for high-quality simulation results was approximately 1/30 of the source wavelength λ. The total domain was 100λ high and long enough to capture a sloping surface with 10λ maximum depth. Perfectly matched layers 1λ deep surrounded the entire simulation to absorb outgoing radiation.

The 2D surface of Fig. 3 can be replaced with any physically realistic rough, lossy, or layered 2D or (with additional computing power) 3D surface, provided bulk dielectric constants are specified. Inhomogeneous distributions of scatterers can be modeled as collections of fine objects, such as dielectric spheres and quads, or by directly specifying a (complex) functional form for the dielectric constant. The scattered radiation field can be computed as the total simulated electric field minus the incident field. To characterize the scattering pattern of randomized targets ensemble averages will be calculated over many simulation runs with statistically similar surfaces.

Analysis pipeline: An input FDTD simulation (or ensemble average over several runs) provides the near-field reflected radiation pattern, but even at periapsis LRO is tens of km above the Moon which is well into the electromagnetic far-field of our meter-scale simulations. A near-to-far-field transformation [9] based on Huygens' principle has been derived and implemented in Matlab, and is currently in testing. This will allow the simulated scattered radiation pattern to be effectively propagated outward to the location of the spacecraft at any desired phase angle β, for any angle of wave incidence. Furthermore, Fig. 4b demonstrates the capability to numerically post-process the refracted subsurface component into individual circular polarizations (via a Jones vector-based Matlab implementation), which will be extended into a full treatment in terms of the Stokes parameters for reflected signals which are commonly used in planetary radar.

Conclusions: We have developed a basic simulation and analysis pipeline for modeling bistatic Mini-RF signals scattered from meter-scale patches at high incidence angles. The simulation setup readily handles near-grazing incidence, which is crucial to modeling polar scattering. Radiation patterns produced by many different physically conceivable surfaces can be simulated, including rough regolith, layers of ice and regolith, and populations of sub-surface scatterers. It is hoped that these simulations will provide new and detailed understanding of the electromagnetic physics behind phase-angle dependencies of backscattered CPR observed in lab observations [4,5] and Mini-RF bistatic images [6]. We are particularly interested in investigating whether apparent changes in CPR β-dependence are uniquely associated with differences in regolith composition (e.g. top-layer ice/regolith scatterer ratios), or if other factors such as surface roughness and stratification also play a major role.

References: [1] Spudis P.D. et al., GRL 2010; [2] Spudis et al. (2013), Icarus, submitted; [3] Bussey D.B.J. et al., LPSC 2013; [4] Hapke et al., 2012; [5] Piatek et al., Icarus 2004; [6] Patterson et al. 2014, LPSC 2014; [7] Fa et al. 2011; [8] Oskooi et al., CPC 2010; [9] Lecture notes by John Schneider, Chapter 14, http://www.eecs.wsu.edu/~schneidj/ufdtd/

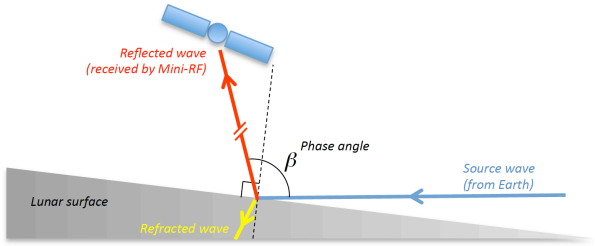

Fig. 1 – Bistatic Mini-RF geometry, with a source wave incident at near-grazing angle upon a polar lunar region; the bistatic angle β is denoted.

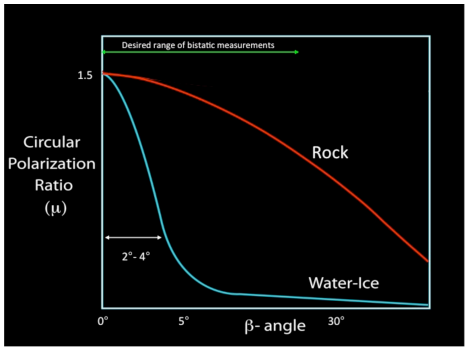

Fig. 2 – Predicted falloff of CPR with increasing bistatic phase angle β for two classes of target surface.

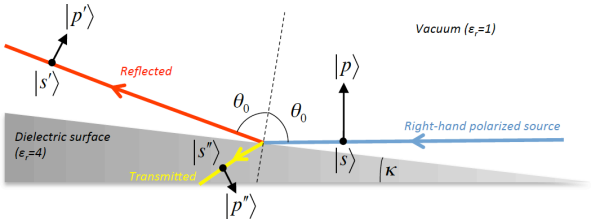

Fig. 3 – Basic 2D simulation setup for testing against Fresnel's equations for reflection and refraction. A right-hand polarized continuous wave is incident at an angle of θ_0 upon a flat dielectric surface. For reference the linear-polarized s- and p- basis vectors (respectively perpendicular and parallel to the plane of incidence) are shown.

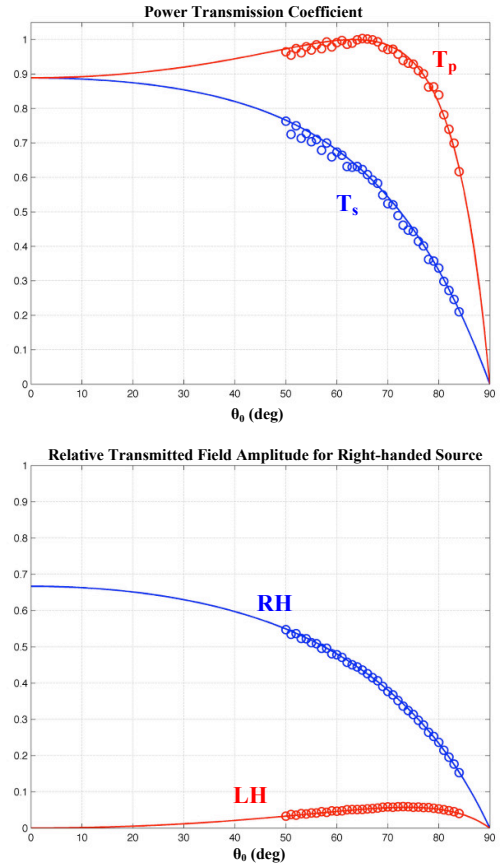

Fig. 4 – FDTD confirmation (circles) of Fresnel's equations (lines) for a range of incidence angles θ_0 on a flat dielectric surface with ε_r=4. (a) Power transmission coefficient for s- and p-components (respectively T_s and T_p). (b) Transmission of right-hand (RH) and left-hand (LH) circularly polarized electric field amplitudes (normalized to incident wave amplitude) for a source plane wave that is purely right-hand circularly polarized.